ACS OMEGA

Open Access

http://pubs.acs.org/journal/acsodf

Article

A First-Principles Study of Graphene and Graphene Oxide as Potential Tamoxifen Drug Delivery Vehicles for Breast Cancer

Suri Wang* and Xuan Luo*

Cite This: *ACS Omega* 2025, 10, 5593−5600

Read Online

ACCESS | Metrics & More | Article Recommendations

ABSTRACT: Targeted therapy with tamoxifen is an effective method to treat breast cancer. This method requires competent drug delivery vehicles to ensure successful therapeutic practices. The stable adsorption between the drug and delivery vehicle is one of the essential components. Using first-principles calculations, the adsorption behaviors of tamoxifen on reduced graphene and graphene oxide were studied based on density functional theory. The results indicated that tamoxifen was weakly adsorbed on pristine graphene, while it was relatively strongly adsorbed on reduced graphene oxides. Our results concluded that among the systems of reduced graphene oxide with an oxygen concentration of 0%, 3.125%, and 12.5%, graphene sheets with oxygen were potential candidates for tamoxifen delivery vehicles for breast cancer targeted therapy, and graphene oxide with an oxygen concentration of 12.5% was the most promising one compared to other carbon-based vehicles.

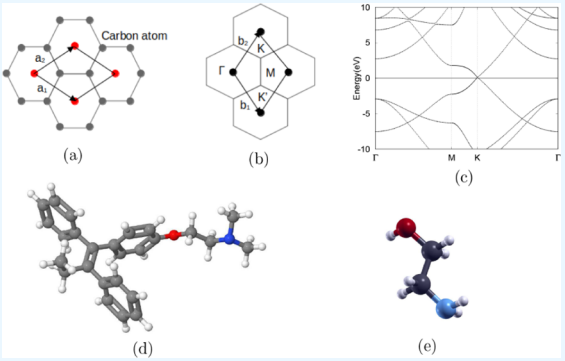

INTRODUCTION

Breast cancer is one of the most prevalent cancers and malignancies in women worldwide.[1] By the start of 2022, approximately 4.1 million women living in the United States were diagnosed with breast cancer, one of the primary reasons for female mortality.[1] It is estimated that 313,510 new breast cancer cases and 42,780 cancer-caused deaths will occur in the year 2024.[2] In its early stages, noninvasive breast cancer has a survival rate of 99% with a five-year treatment.[3] However, the metastatic and invasive stages of breast cancer are challenging to cure with the spread of tumors to distant organs, such as the brain, liver, lung, and bone.[3,4] Accordingly, the high mortality rate of invasive breast cancer is most likely due to a lack of specific targeting. In response to this issue, targeted therapy has gained increased attention and is an important component among other treatments such as chemotherapy and radiotherapy.[5−7] Since targeted therapy works by targeting cancer-treating agents to the area around the tumor or the patient's whole body,[8] it is crucial to perform effective and safe drug delivery processes, which is essential to subsequent treatments.

Tamoxifen is a selective estrogen receptor modulator that is effective and affordable in breast cancer targeted therapy.[9,10] It functions by preventing estrogen and estradiol from binding with the estrogen receptor of breast tissues, thus inhibiting the overproduction of estrogen and slowing tumor growth.[11−13] However, the prolonged use of tamoxifen faces some challenges, such as endometrial cancer, thromboembolisms, and menopausal symptoms.[14−16] Considering these challenges, the development of novel and effective delivery methods that balance the dose is increasingly important.[12,17]

In the face of the challenges caused by traditional targeted therapy, nanotechnology has demonstrated promising improvements in the delivery of therapeutic agents.[18−21] For example, by modifying the size, shape, chemical properties, and physical properties of nanoparticles, scientists are able to target desired cells.[8] Nanocarriers are also capable of carrying modest amounts of drugs to tumors for an extended period of time, limiting the dose-dependent toxicity.[22,23] Moreover, as a carbon-based material, nanodiamond application in previous studies demonstrated medical relevance resulting from their biological applications and their physical and chemical properties, including stability, scalability, biocompatibility, small size, and good adsorption.[24,25]

Landeros-Martinez et al. connected nanodiamonds with a variety of polymers, including 2-hydroxypropanal, polyethylene glycol, and polyglycolic acid, to successfully deliver bioagents through the circulatory system.[11,26] Additionally, graphene oxide nanoparticles and nanodiamonds have been tested as potential drug delivery vehicles.[17,27,28] However, under the same

Received: September 16, 2024
Revised: January 19, 2025
Accepted: January 22, 2025
Published: February 3, 2025

volume, monolayers have a higher surface area compared to nanodiamonds. This puts nanodiamonds at a disadvantage since their atoms are packed in a prism instead of being spread out and creating more binding sites, like those in a monolayer, which makes it very stable and strong as a drug carrier. In addition, the small size and carbon-based composition of graphene layers, which contribute to their biocompatibility, low toxicity, and safety in the human body, have been extensively investigated as potential drug delivery vehicles for various drugs and therapeutic applications targeting different diseases.[29,30] These materials have shown promise due to their unique properties, including high surface area, tunable surface chemistry, and the ability to effectively load and release therapeutic agents within biological systems. The delivery of tamoxifen using graphene oxide nanocarriers is viable, as the drug loading capacity of 1.7 mg of tamoxifen per mg of graphene oxide with a 90% loading efficiency allows for the efficient delivery of the recommended daily dose of 20−40 mg.[9,31] With graphene oxide carriers optimized to fall within the ideal size range of 30−200 nm for effective retention in blood vessels and tumor targeting, the system ensures adequate drug loading and controlled release, making it a promising strategy for treating metastatic breast cancer.[32] Therefore, we further investigated reduced graphene and graphene oxide with different oxygen concentrations as potential tamoxifen delivery vehicles for the targeted therapy of breast cancer.

We performed first-principles calculations to determine adsorption energy, band structure, and charge transfer on tamoxifen adsorbed on reduced graphene and graphene oxides. To elucidate the binding mechanism of tamoxifen with graphene and graphene oxide layers, we conducted a series of band structure, charge transfer, density of states, and projected density of states calculations. These analyses aim to assess the influence of the additional oxygen atoms on the drug−vehicle interactions and to identify the source of the adsorption energy. The results concerning adsorption energy and electronic structure, as presented in this study, offer valuable theoretical insights into the adsorption behavior of TAM on graphene and graphene oxide surfaces.[33] In the second section, we detail our theoretical methods. In the third section, we present our results and discussions on tamoxifen adsorbed on graphene and graphene oxide configurations. We also compare our results with those of other theoretical research. Finally, our conclusion can be found in the fourth section.

METHOD

Computational Details. First-principles calculations were performed based on density functional theory (DFT) using the generalized gradient approximation (GGA) in the format of Perdew−Burke−Ernzerhof (PBE)[34] implemented in the Abinit code.[35] The projector-augmented wave (PAW) method[36,37] was used to produce the pseudopotentials of the elements studied, including carbon, hydrogen, oxygen, and nitrogen. The valence electron configuration and radius cutoff for the elements used in this study are listed in Table 1.

In each self-consistent field (SCF) iteration, the process was considered converged when the total energy difference of data sets was less than 1.0×10^{-10} hartree. By performing total energy calculations of multiple data sets, the kinetic energy cutoff, Monkhorst−Pack k-point grid, and vacuum heights were considered converged after the total energy difference was less than 0.0001 hartree (about 3 meV) twice consecutively.

Table 1. Electron Configuration and Radius Cut-Off of Elements Used in This Study for Generation of PAW Pseudopotential

Elements	Electron configuration	Radius cutoff (bohr)
Hydrogen (H)	$1s^1$	1.00
Carbon (C)	$[He]2s^22p^2$	1.51
Oxygen (O)	$[He]2s^22p^4$	1.41
Nitrogen (N)	$[He]2s^22p^3$	1.20

Atomic Structures. Graphene was first relaxed in a 1×1 primitive cell, as shown in Figure 1. A 4×4 graphene supercell (G44) was then relaxed, as shown in Figure 2a. The relaxation iterations were considered to be converged when the maximum absolute force on each atom was less than 2.0×10^{-4} hartree $bohr^{-1}$ (about 0.01 eV/Å). The kinetic energy cutoff, Monkhorst−Pack k-point grid values, and vacuum layer were calculated for the elements used in this study. The vacuum layers of the tamoxifen drug and graphene monolayers were converged separately. Subsequently, the corresponding values were combined to obtain the vacuum layer for the drug-carrier system, while ensuring an additional buffer space, preserving the integrity of the individual systems.

Then, we structured different concentrations of oxygen on the surface of a 4×4 graphene supercell to determine the optimal structure for drug delivery. In this study, we considered an idealized situation involving free-standing reduced graphene oxide layers—an infinitely large sheet devoid of edges or with edges positioned beyond practical influence. Moreover, while the role of graphene oxide edges in electrochemical activity is well-recognized,[38] most current studies primarily focus on utilizing the surface of graphene oxide due to its larger contact area and its advantages specific to each drug application.[39] Therefore, considering the previously mentioned reason and recognizing that an in-depth exploration of the edges of graphene oxide may fall outside the scope of the current study, we have centered our investigation on the surface of graphene oxide.

By reducing 4×4 graphene sheets with one oxygen (GO1) and four oxygens (GO4), we obtained reduced graphene oxide monolayers with 3.125% and 12.5% oxygen concentrations, respectively, which are shown in Figure 2b,c. The above systems and configurations of oxygen atoms, including that of GO4, were selected for evaluation based on their demonstrated adsorption properties as reported in previous therapeutic studies.[40] Our current configuration of GO4 exhibits the lowest energy in previous studies, thereby demonstrating the highest stability, making it suitable for further analysis. Furthermore, no graphene oxide systems with oxygen concentrations above 12.5% were evaluated to determine if adsorption energy increased. This is because reduced graphene oxide was shown to have an atomic oxygen concentration of approximately 10.7%.[41] Additionally, a higher adsorption energy can increase the likelihood of the drug binding tightly to its carriers, which could potentially hinder its detachment at the intended site of action. This risk means that while strong adsorption is beneficial for keeping the drug bound to the vehicle during delivery, overly strong binding may reduce the drug's bioavailability or effectiveness if it cannot detach and be released when it reaches the target tissue. Then, the full relaxation was carried out, and the optimized atomic configurations were obtained for GO1 and GO4.

The tamoxifen (TAM) molecule shown in Figure 1d was truncated, with only the reactive part kept in our study. The

https://doi.org/10.1021/acsomega.4c08517
ACS Omega 2025, 10, 5593−5600

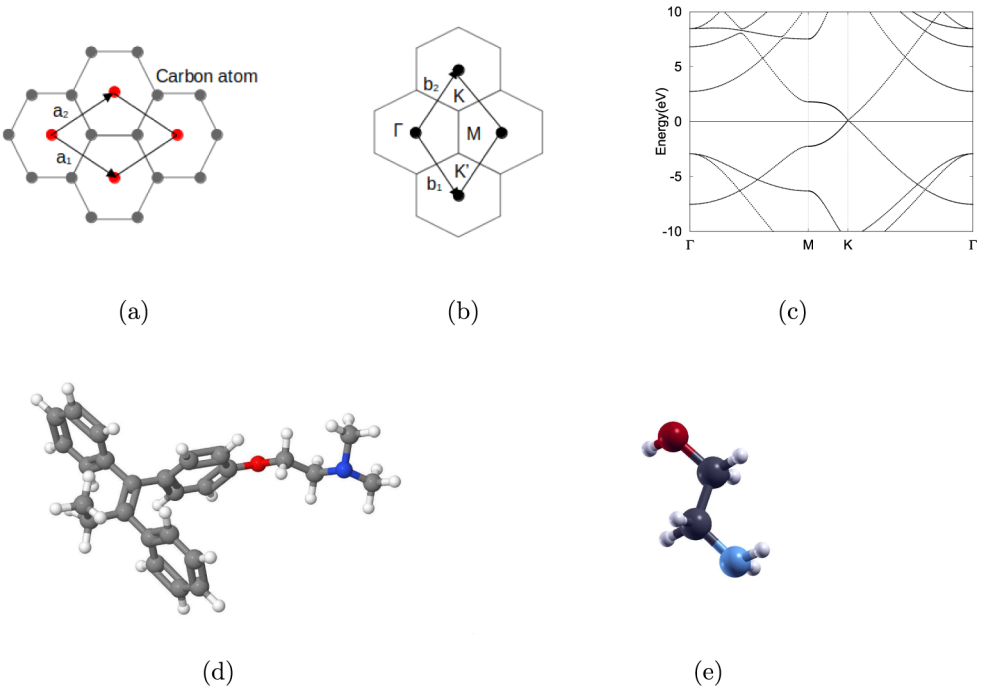

Figure 1. (a) Graphene primitive cell a_1 and a_2 represent the lattice vector. (b) Graphene first Brillouin zone b_1 and b_2 represent the wave vector. The high-symmetry k-points are Γ, K, K', and M. (c) Graphene primitive cell band structure. 0 eV is the Fermi level. (d) 3D molecular structure of the tamoxifen drug. (e) 3D molecular structure of the truncated tamoxifen drug. Carbon, hydrogen, oxygen, and nitrogen atoms are represented by gray, white, red, and blue, respectively.

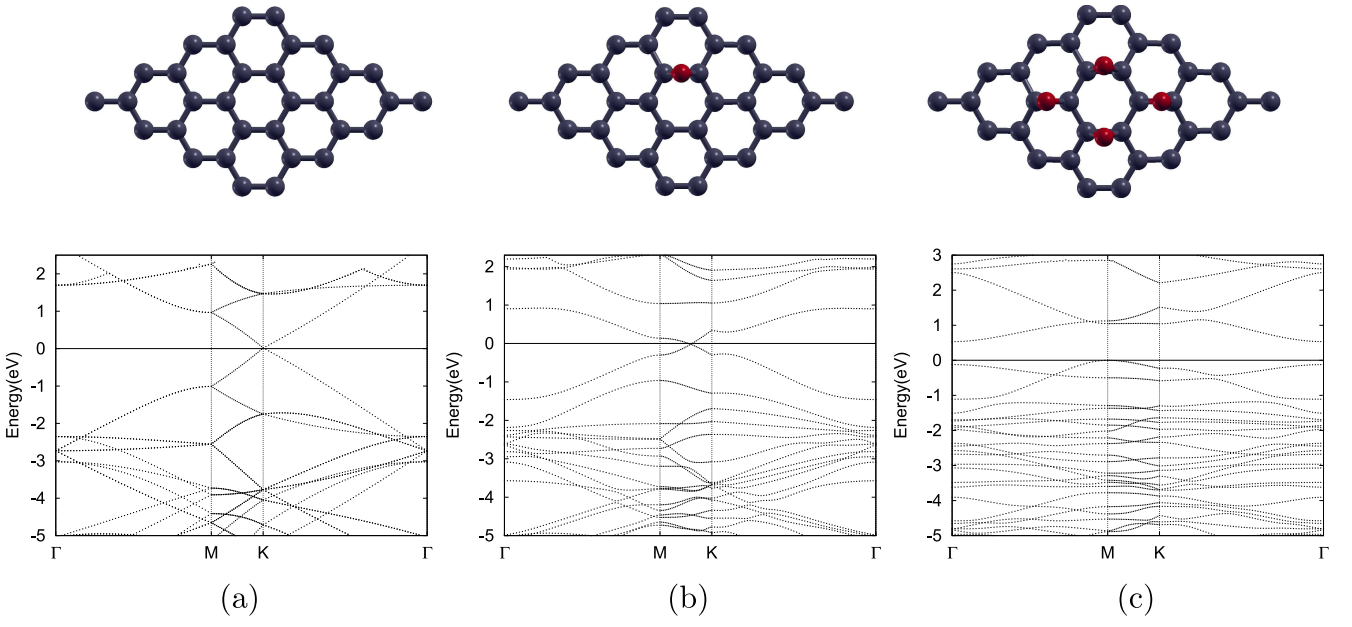

Figure 2. Optimized atomic structure and band structure of (a) 4 × 4-graphene, (b) one oxygen-doped 4 × 4-graphene, and (c) four oxygen-doped 4 × 4-graphene. Carbon and oxygen atoms are represented as gray and red respectively.

structure of the truncated molecule was then fully relaxed, as shown in Figure 1e. After that, TAM was adsorbed with the amino functional group (NH2) closest to fully optimized graphene and graphene oxide monolayers. NH2 is positioned closer to the reduced graphene sheets because carbon rings attached to the hydroxyl functional group may hinder the adsorption of the molecules. The atomic structure of the combined complex was then optimized, as shown in Figure 3.

Adsorption Energy. The adsorption energy of the TAM molecule on graphene and graphene oxides was calculated to determine whether there was an attraction between the molecule and the monolayer that enabled drug delivery. The adsorption energy was obtained according to the following equation:

$$E_{ad} = E_{ml+tam} - E_{ml} - E_{tam} \quad (1)$$

https://doi.org/10.1021/acsomega.4c08517
ACS Omega 2025, 10, 5593−5600

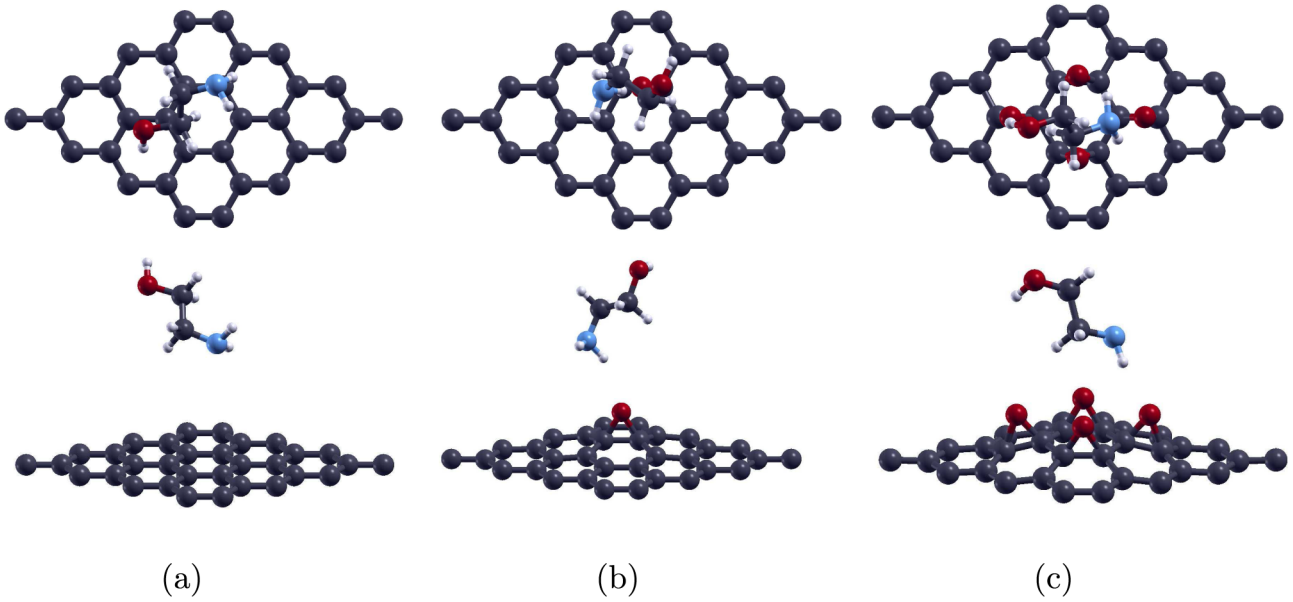

Figure 3. Top view and side view of (a) tamoxifen adsorbed on 4 × 4-graphene, (b) tamoxifen adsorbed on one oxygen-doped 4 × 4-graphene, and (c) tamoxifen adsorbed on four oxygen-doped 4 × 4-graphene. Carbon, hydrogen, oxygen, and nitrogen atoms are represented by gray, white, red, and blue, respectively.

where E_{ad} is the adsorption energy, E_{ml+tam} is the total energy of the complex consisting of TAM and the monolayer, E_{ml} is the total energy of the monolayer, and E_{tam} is the total energy of the drug molecule TAM. A negative value indicates that the system is exothermic, whereas a positive value indicates that the system is endothermic. Therefore, a more negative adsorption value indicates that the system is more stable.

Electron Structure. The band structure calculations of the monolayers and the molecule-monolayer-formed complex were performed. The high-symmetry k-point circuits were Γ (0.0, 0.0, 0.0), M (1/2, 1/2, 0.0), and K (1/3, 2/3, 0.0).

We then investigated the electronic structural properties of the total density of states (DOS) and projected density of states (PDOS) of the systems. The tetrahedron method was used to calculate the DOS and PDOS of TAM adsorbed on pure graphene and graphene oxide monolayers. The atoms chosen for PDOS were the atoms closest to the site of adsorption, which include the 1s orbital of hydrogen, the 2p orbital of oxygen, the 2p orbital of carbon, and the 2p orbital of nitrogen, depending on the different configurations.

We also evaluated the charge difference before and after the drug molecule was adsorbed onto the monolayers. The charge transfer was calculated using the following equation:

$$\Delta\rho(r) = \rho_{ml/tam}(r) - \rho_{ml}(r) - \rho_{tam}(r) \quad (2)$$

where $\Delta\rho(r)$ represents the charge transfer, $\rho_{ml+tam}(r)$ denotes the charge density of the drug molecule adsorbed onto the monolayers, $\rho_{ml}(r)$ represents the charge density of the monolayers, and $\rho_{tam}(r)$ gives the charge density of the drug molecule TAM.

RESULTS AND DISCUSSIONS

To study whether the monolayers can serve as a drug delivery vehicle, we evaluated the atomic structure, band structure, adsorption energy, charge transfer, and total DOS and PDOS of TAM adsorbed on pure graphene or graphene oxide monolayers.

Pure Materials. TAM molecule was truncated to improve computational efficiency. The structure of the truncated TAM is displayed in Figure 1e. The relaxed bond lengths were 0.97 Å for H−O, 1.43 Å for O−C, 1.1 Å for C−H, and 1.02 Å for N−H. The converged kinetic energy cutoff was 20 hartree for carbon, 20 hartree for oxygen, 25 hartree for hydrogen, and 26 hartree for nitrogen. We then took the maximum energy cutoff of the elements in each system. The converged vacuum range for oxygen was 10 bohr. The converged value of vacuum height was 13 bohr for 1 × 1 graphene. The k-point grid was 14 × 14 × 1 for 1 × 1 graphene unit cell.

A 4 × 4 graphene monolayer was constructed as shown in Figure 2a. The obtained lattice constant for G44 was 18.61 bohr. Our result is consistent with previous calculations, which recorded a lattice constant of 18.56 bohr.[42] In the band structure shown in Figure 2a, the Dirac point for G44 is located on the high-symmetry k-point K.

Graphene Oxide. In contrast to substitutional doping, our study investigates interstitial doping, where one or four oxygen atoms are positioned at the bridge site of the carbon−carbon bond within the graphene sheet. These configurations correspond to oxygen concentrations of 3.125% and 12.5%, respectively. Figure 2 displays the successfully relaxed configuration of graphene oxide along with its band structures.

Figure 2b shows the optimized atomic and band structures of GO1. The oxygen atom was placed on the bridge site above the bond between the carbon atoms as shown. This bridge site was chosen because previous studies have proved that it is an energy-favorable location.[43,44] The converged lattice constant for GO1 was 18.67 bohr. In the band structure, the Dirac point for GO1 shifts between high-symmetry k-points M and K.

Figure 2c shows the atomic and band structures of GO4. Four oxygens were interstitially placed on the four bridge sites around the hexagon, as shown in the top figure of Figure 2c. The converged lattice constant for GO4 was 18.72 bohr. Thus, the lattice constants of GO1 and GO4 are slightly larger than that of pristine graphene. This is typically due to the additional space occupied by the oxygen atoms and distortion from different

https://doi.org/10.1021/acsomega.4c08517
ACS Omega 2025, 10, 5593−5600

bond angles and bond lengths.[45−47] There is a direct band gap at the high symmetry K point of GO4, as shown in the bottom figure of Figure 2c.

Drug Molecule Adsorption. The interactions between TAM and graphene or graphene oxide monolayers were investigated. TAM was adsorbed on top of G44, GO1, and GO4 monolayers, forming G44TAM, GO1TAM, and GO4TAM complexes, respectively, as illustrated in Figure 3. TAM was placed at the center of the graphene sheet or on top of the oxygen atoms of the graphene oxide sheets to maximize potential adsorption.

The adsorption energy for each system was calculated using eq 1. Previous studies have reported adsorption energies for graphene oxide ranging from approximately −20 kcal/mol to −100 kcal/mol (approximately −0.032 to −0.16 Ha).[40,48] The adsorption energy observed in our study is 1 order of magnitude smaller than those reported in earlier research; however, this finding is consistent with our theoretical rationale. Specifically, we propose that low adsorption energies may hinder drug uptake, while excessively high adsorption energies could impede drug release within the human body. Thus, the calculated adsorption energy in our study is in a very reasonable range and will not result in adsorption difficulties.

To further investigate the adsorption properties of TAM on different monolayers, we carried out the band structure calculations of G44TAM, GO1TAM, and GO4TAM, as shown in Figure 4. We also calculated the DOS and PDOS values, as shown in Figures 4 and 5. Using our total energy calculations, we plotted charge transfer in each interface, as shown in Figure 5. Charge densities for the interface, isolated surface, and isolated molecule were obtained from total energy calculations. Charge transfer was calculated according to eq 2. The blue regions represent electron acceptors, and the pink regions represent electron donors. Charge is transferred from areas of depletion to areas of accumulation.

Tamoxifen on Pure Graphene. TAM was adsorbed onto the center of the G44 monolayer. Figure 3a exhibits the atomic structure of G44TAM, and Table 2 shows the lattice constant and adsorption distance.

The band structure of G44TAM contains a Dirac point meeting at the high-symmetry k-point K, as shown in Figure 4a. The valence band maximum (VBM) meets the conduction band minimum (CBM) at the Fermi level, showing a 0 direct band gap. The band structures of G44TAM and G44 are similar, indicating that the addition of TAM does not affect the band structure of G44 significantly.

The calculated binding energy of the complex was 0.0035 Ha, as shown in Table 2. The positive adsorption energy indicates that the interaction between the drug and the carrier is unfavorable. Since the drug cannot spontaneously adsorb onto the carrier, energy input is required for adsorption to occur, suggesting that modification of the monolayer to facilitate adsorption could be a worthwhile strategy. Nonetheless, there exists physisorption between TAM and G44 in reality. Consequently, we conducted experiments using modified carriers, which exhibited energy-favorable interactions. This observation of positive adsorption energy is consistent with findings from previous studies that investigated materials similar to graphene as a drug carrier.[49,50]

The charge transfer of G44TAM is shown in Figure 5a. Structure G44TAM has an isosurface value of 0.0002 e/Bohr^3. The weak interaction between TAM and G44 was further confirmed by the charge transfer of the G44TAM system. It is

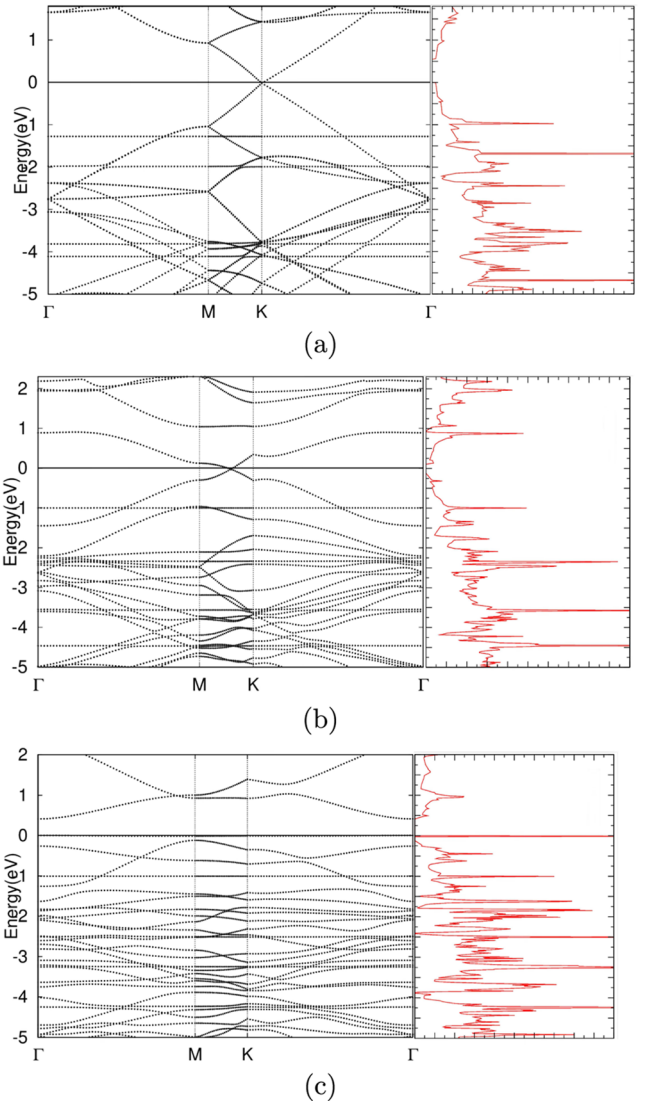

Figure 4. Band structure and total DOS of (a) tamoxifen adsorbed on 4 × 4-graphene, (b) tamoxifen adsorbed on one oxygen-doped 4 × 4-graphene, and (c) tamoxifen adsorbed on four oxygen-doped 4 × 4-graphene. 0 eV is the Fermi level.

observed that there is no overlap of blue and pink regions, implying that there was barely any electron movement occurring in the interface region.

The PDOS of the G44TAM system, shown in Figure 5a, shows the fewest peaks among the three systems. In G44TAM, there are overlapping peaks around −3.5 eV between H 1s, O 2p, and N 2p orbitals. However, the hybridization of these orbitals is not obvious, indicating a weak interaction between TAM and G44. The calculated results of PDOS are in agreement with the obtained small value of adsorption energy for G44TAM.

Tamoxifen on Graphene Oxide with Oxygen Concentration 3.125%. TAM was adsorbed on the GO1 monolayer, as shown in Figure 3b. The lattice constant and adsorption distance are shown in Table 2. The complex was fully relaxed, and its total energy was achieved.

The band structure of GO1TAM contains a Dirac point meeting between high-symmetry k-points M and K. There is a 0 direct band gap as the VBM meets the CBM at the Fermi level.

The calculated binding energy of GO1TAM was −0.0002 Ha, as shown in Table 2. GO1TAM displays negative adsorption

https://doi.org/10.1021/acsomega.4c08517
ACS Omega 2025, 10, 5593−5600

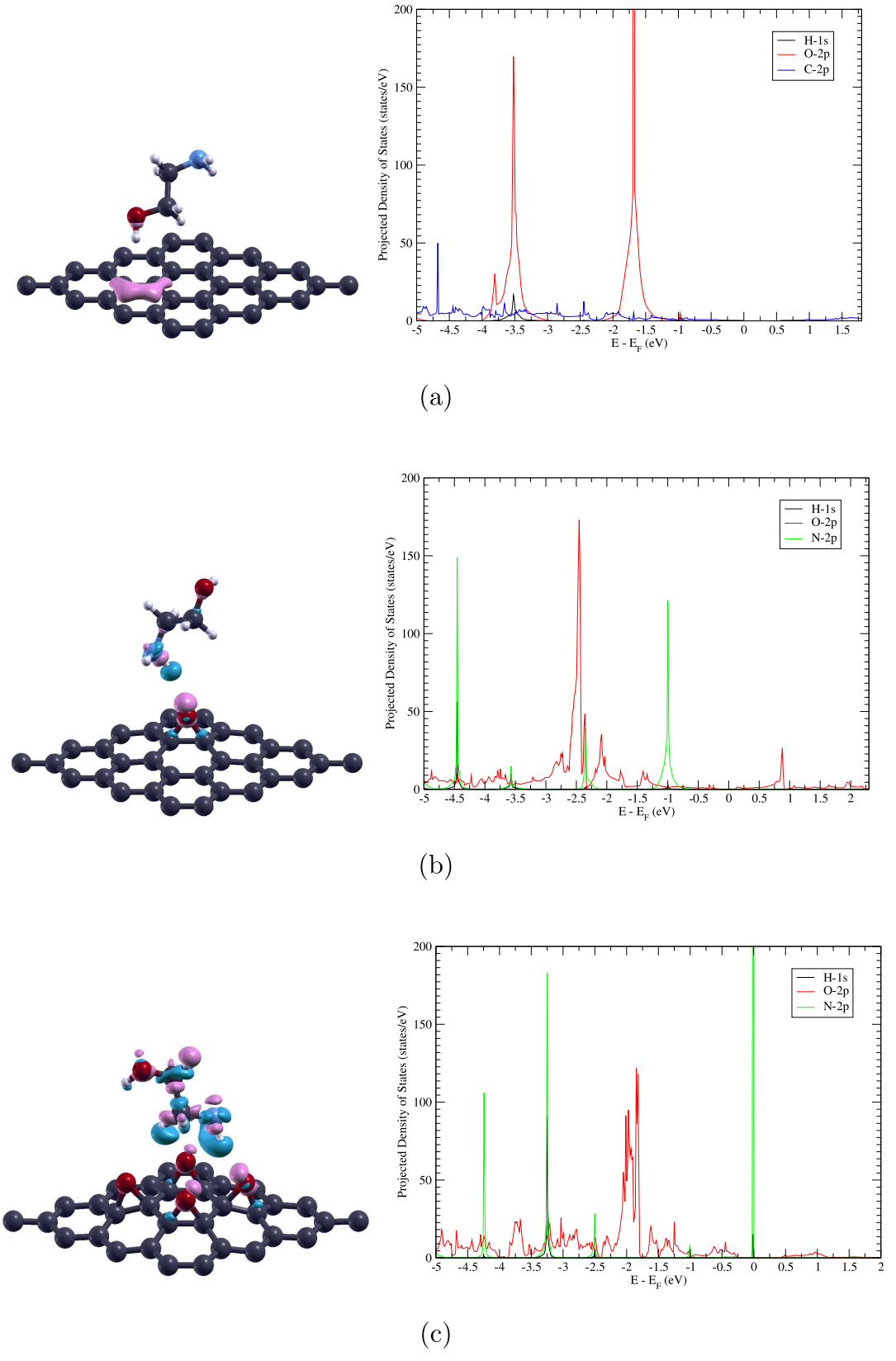

Figure 5. Charge transfer and PDOS of (a) tamoxifen adsorbed on 4 × 4-graphene with isovalue = 0.0002 e/Bohr^3, (b) tamoxifen adsorbed on one oxygen-doped 4 × 4-graphene with isovalue = 0.001 e/Bohr^3, and (c) tamoxifen adsorbed on four oxygen-doped 4 × 4-graphene with isovalue = 0.007 e/Bohr^3. Carbon, hydrogen, oxygen, and nitrogen atoms are represented by gray, white, red, and blue, respectively. Carbon, hydrogen, oxygen, and nitrogen orbitals are represented by blue, black, red, and green lines, respectively.

energy, indicating a stronger attraction between the molecule and the monolayer compared to G44TAM. This finding is consistent with studies with similar methods.[51] There was no bonding observed between TAM and GO1; instead, charge

https://doi.org/10.1021/acsomega.4c08517
ACS Omega 2025, 10, 5593−5600

Table 2. Adsorption Energy (E_{ad}) in Ha, Adsorption Energy (E_{ad}) in eV, Lattice Constant (a) in Bohr, and Adsorption Distance (E_{ad} d) in Bohr between Graphene Monolayers and Tamoxifen

Complex	E_{ad} (Ha)	E_{ad} (eV)	a (bohr)	E_{ad} d (bohr)
G44TAM	0.0035	0.096	18.64	6.07
GO1TAM	−0.0002	−0.007	18.67	4.89
GO4TAM	−0.0033	−0.089	18.72	5.08

transfer observed between the drug molecule and the graphene oxide sheet indicates the exchange of electrons.

Charge transfer of GO1TAM was calculated to examine the change in electron density distribution resulting from interactions between GO1 and TAM, as shown in Figure 5b. The isosurface value of this structure is 0.001 e/Bohr^3. There was an improvement in the overlap between the blue and pink regions, indicating a stronger adsorption at the interface. The charge accumulates in the region of the oxygen atom of GO1 and the hydrogen atom of TAM.

As shown in Figure 5b, the PDOS of the GO1TAM system shows more peaks compared to those of G44TAM, displaying a stronger interaction between the molecule and the monolayer. In GO1TAM, there are overlapping peaks around −4.5 eV between H 1s, O 2p, and N 2p orbitals, indicating hybridization. The highest peak is shown at −2.5 eV of O 2p orbitals.

TAM on Graphene Oxide with Oxygen Concentration 12.5%. The TAM molecule was adsorbed on GO4, as shown in Figure 3c. Its lattice constant and adsorption distance are shown in Table 2.

After optimization, the band structure of GO4TAM was calculated, as shown in Figure 4c. The band structure has a direct band gap, as the VBM and the CBM are at the same high-symmetry k-point near point K. With a smaller band gap, GO4TAM exhibits more localized electronic states near the Fermi level, which can enhance interactions with adsorbates, such as tamoxifen. The reduced band gap in the system is due to GO's oxygen-functionalized surface, which is capable of facilitating charge transfer between the carrier and the drug. This charge transfer can contribute to stronger adsorption energies. Additionally, the carrier's ability to donate or accept electrons further enhances the binding affinity between the drug and the material.

The computed binding energy of optimized GO4TAM was −0.0033 Ha, as shown in Table 2. There is no bonding observed between TAM and GO4; however, there is also charge transfer between the components. Among the three graphene systems, GO4TAM demonstrates the most negative adsorption energy, suggesting it is the best adsorption structure for TAM.

Charge transfer of GO4TAM is shown in Figure 5c. The structure GO4TAM has an isosurface value of 0.0007 e/Bohr^3. There is considerable charge accumulation on the four oxygen atoms on the monolayer and the hydrogen atoms of TAM. The charge transfer demonstrates chemisorption, indicated by the overlapping between the blue and pink regions, which shows the exchange of electrons between TAM and the oxygen atoms of GO4. This is consistent with our previous E_{ad} calculation and confirms relatively strong interactions between the molecule and the graphene layer.

Compared to that of G44TAM, the PDOS of the GO4TAM system also shows more peaks. In GO4TAM, there are overlapping peaks shown at around −3.25 and −2.5 eV between H 1s and N 2p orbitals, indicating hybridization and interactions between TAM and GO4.

CONCLUSION

In summary, by using first-principles calculations based on density functional theory, the adsorption behavior of tamoxifen adsorbed on pure graphene and graphene oxides was investigated. The obtained results of the adsorption distance, adsorption energy, and charge transfer indicated that tamoxifen was weakly adsorbed on pure graphene, while it was relatively strongly adsorbed on graphene oxide. Considering the calculated results for electronic properties, it can be concluded that graphene oxides are potential candidates for drug delivery vehicles, and graphene oxide with a 12.5% oxygen concentration is the most promising one. However, reduced graphene oxide has a limited oxygen concentration, which constrains its ability to interact effectively with drugs. Moreover, excessively high adsorption energy between the drug and carrier may lead to difficulties in desorption, hindering the controlled release of the drug. Therefore, doping graphene sheets with additional functional groups, such as hydroxyl groups, can be a viable strategy to enhance the interaction between the drug and carrier while maintaining optimal adsorption and desorption characteristics.

AUTHOR INFORMATION

Corresponding Authors

Suri Wang − *National Graphene Research and Development Center, Springfield, Virginia 22151, United States;* orcid.org/0009-0000-8503-2375; Email: suri.wang2006@gmail.com

Xuan Luo − *National Graphene Research and Development Center, Springfield, Virginia 22151, United States;* orcid.org/0000-0002-0592-0610; Email: xluo@ngrd.org

Complete contact information is available at: https://pubs.acs.org/10.1021/acsomega.4c08517

Notes

The authors declare no competing financial interest.

ACKNOWLEDGMENTS

We would like to thank Dr. Geifei Qian for providing technological support. There was no financial assistance received for this study.

REFERENCES

(1) Giaquinto, A. N.; Sung, H.; Miller, K. D.; Kramer, J. L.; Newman, L. A.; Minihan, A.; Jemal, A.; Siegel, R. L. Breast cancer statistics, 2022. *Ca-Cancer J. Clin.* **2022**, *72*, 524−541.

(2) Siegel, R. L.; Giaquinto, A. N.; Jemal, A. Cancer statistics, 2024. *Ca-Cancer J. Clin.* **2024**, *74* (1), 12−49.

(3) Akram, M.; Iqbal, M.; Daniyal, M.; Khan, A. U. Awareness and current knowledge of breast cancer. *Biol. Res.* **2017**, *50* (1), 33.

(4) Sun, Y.-S.; Zhao, Z.; Yang, Z.-N.; Xu, F.; Lu, H.-J.; Zhu, Z.-Y.; Shi, W.; Jiang, J.; Yao, P.-P.; Zhu, H.-P. Risk factors and preventions of breast cancer. *Int. J. Biol. Sci.* **2017**, *13*, 1387.

(5) Waks, A. G.; Winer, E. P. Breast cancer treatment: a review. *JAMA* **2019**, *321*, 288−300.

(6) Burguin, A.; Diorio, C.; Durocher, F. Breast cancer treatments: updates and new challenges. *J. Pers. Med.* **2021**, *11*, 808.

(7) Higgins, M. J.; Baselga, J. Targeted therapies for breast cancer. *J. Clin. Invest.* **2011**, *121*, 3797−3803.

https://doi.org/10.1021/acsomega.4c08517
ACS Omega 2025, 10, 5593−5600

(8) Sutradhar, K. B.; Amin, M. L. Nanotechnology in cancer drug delivery and selective targeting. *Int. Scholarly Res. Not.* **2014**, *2014*, 939378.
(9) Farrar, M. C.; Jacobs, T. F. *Tamoxifen*; StatPearls Publishing: Treasure Island (FL), 2018.
(10) O'Regan, R. M.; Jordan, V. C. The evolution of tamoxifen therapy in breast cancer: selective oestrogen-receptor modulators and down-regulators. *Lancet Oncol.* **2002**, *3*, 207−214.
(11) Landeros-Martinez, L.-L.; Glossman-Mitnik, D.; Orrantia-Borunda, E.; Flores-Holguín, N. New methods of esterification of nanodiamonds in fighting breast cancer−a density functional theory approach. *Molecules* **2017**, *22*, 1740.
(12) Sani, A.; Pourmadadi, M.; Shaghaghi, M.; Eshaghi, M. M.; Shahmollaghamsary, S.; Arshad, R.; Fathi-Karkan, S.; Rahdar, A.; Medina, D. I.; Pandey, S. Revolutionizing anticancer drug delivery: Exploring the potential of tamoxifen-loaded nanoformulations. *J. Drug Delivery Sci. Technol.* **2023**, *86*, 104642.
(13) Lee, Y. T.; Tan, Y. J.; Oon, C. E. Molecular targeted therapy: Treating cancer with specificity. *Eur. J. Pharmacol.* **2018**, *834*, 188−196.
(14) Mourits, M. J.; De Vries, E. G.; Willemse, P. H.; Ten Hoor, K. A.; Hollema, H.; Van der Zee, A. G. Tamoxifen treatment and gynecologic side effects: a review. *Obstet. Gynecol.* **2001**, *97*, 855−866.
(15) Lorizio, W.; Wu, A. H.; Beattie, M. S.; Rugo, H.; Tchu, S.; Kerlikowske, K.; Ziv, E. Clinical and biomarker predictors of side effects from tamoxifen. *Breast Cancer Res. Treat.* **2012**, *132*, 1107−1118.
(16) Love, R. R.; Cameron, L.; Connell, B. L.; Leventhal, H. Symptoms associated with tamoxifen treatment in postmenopausal women. *Arch. Intern. Med.* **1991**, *151* (9), 1842−1847.
(17) Lila, A. S. A.; Soliman, M. S.; Kiran, H. C.; Gangadharappa, H. V.; Younes, K. M.; Khafagy, E.-S.; Shehata, T. M.; Ibrahim, M. M.; Abdallah, M. H. Tamoxifen-loaded functionalized graphene nanoribbons for breast cancer therapy. *J. Drug Delivery Sci. Technol.* **2021**, *63*, 102499.
(18) Li, Y.; Humphries, B.; Yang, C.; Wang, Z. Nanoparticle-mediated therapeutic agent delivery for treating metastatic breast cancer−challenges and opportunities. *Nanomaterials* **2018**, *8*, 361.
(19) He, L.; Yu, A.; Deng, L.; Zhang, H. Eradicating the roots: advanced therapeutic approaches targeting breast cancer stem cells. *Curr. Pharm. Des.* **2020**, *26*, 2009−2021.
(20) Napier, M. E.; DeSimone, J. M. Nanoparticle drug delivery platform. *J. Macromol. Sci., Polym. Rev.* **2007**, *47*, 321−327.
(21) Saeed, N.; Hamzah, I.; Mahmood, S. The applications of nanomedicine in the breast cancer therapy. *J. Phys.: Conf. Ser.* **2021**, *1853*, 012061.
(22) Maji, R.; Dey, N. S.; Satapathy, B. S.; Mukherjee, B.; Mondal, S. Preparation and characterization of Tamoxifen citrate loaded nanoparticles for breast cancer therapy. *Int. J. Nanomed.* **2014**, *9*, 3107−3118.
(23) de Kozak, Y.; Andrieux, K.; Villarroya, H.; Klein, C.; Thillaye-Goldenberg, B.; Naud, M.-C.; Garcia, E.; Couvreur, P. Intraocular injection of tamoxifen-loaded nanoparticles: a new treatment of experimental autoimmune uveoretinitis. *Eur. J. Immunol.* **2004**, *34*, 3702−3712.
(24) Man, H. B.; Ho, D. Nanodiamonds as platforms for biology and medicine. *J. Clin. Lab. Autom.* **2013**, *18*, 12−18.
(25) Mostofizadeh, A.; Li, Y.; Song, B.; Huang, Y. Synthesis, properties, and applications of low-dimensional carbon-related nanomaterials. *J. Nanomater.* **2011**, *2011*, 685081.
(26) Khandare, J.; Calderón, M.; Dagia, N. M.; Haag, R. Multifunctional dendritic polymers in nanomedicine: opportunities and challenges. *Chem. Soc. Rev.* **2012**, *41*, 2824−2848.
(27) Zhang, Y.-j.; Li, B.-a.; Li, Z.-y.; Yu, H.-y.; Zhang, Y.-z. Synthesis and characterization of Tamoxifen citrate modified reduced graphene oxide nano sheets for breast cancer therapy. *J. Photochem. Photobiol., B* **2018**, *180*, 68−71.
(28) Keklikcioglu Cakmak, N.; Eroglu, A. Doxorubicin and tamoxifen loaded graphene oxide nanoparticle functionalized with chitosan and folic acid for anticancer drug delivery. *Polym. Bull.* **2023**, *80*, 2171−2185.
(29) Liu, J.; Cui, L.; Losic, D. Graphene and graphene oxide as new nanocarriers for drug delivery applications. *Acta Biomater.* **2013**, *9*, 9243−9257.
(30) Jiang, J.-H.; Pi, J.; Jin, H.; Cai, J.-Y. Functional graphene oxide as cancer-targeted drug delivery system to selectively induce oesophageal cancer cell apoptosis. *Artif. Cells, Nanomed., Biotechnol.* **2018**, *46*, 297−307.
(31) Sharma, H.; Mondal, S. Functionalized graphene oxide for chemotherapeutic drug delivery and cancer treatment: a promising material in nanomedicine. *Int. J. Mol. Sci.* **2020**, *21*, 6280.
(32) Oliveira, A. M.; Machado, M.; Silva, G. A.; Bitoque, D. B.; Tavares Ferreira, J.; Pinto, L. A.; Ferreira, Q. Graphene oxide thin films with drug delivery function. *Nanomaterials* **2022**, *12*, 1149.
(33) Zhou, L.; Zhu, H.; Zeng, W. Density functional theory study on the adsorption mechanism of sulphide gas molecules on α-Fe2O3 (001) surface. *Inorganics* **2021**, *9*, 80.
(34) Perdew, J. P.; Burke, K.; Ernzerhof, M. Generalized gradient approximation made simple. *Phys. Rev. Lett.* **1996**, *77*, 3865.
(35) Gonze, X.; Amadon, B.; Anglade, P.-M.; Beuken, J.-M.; Bottin, F.; Boulanger, P.; Bruneval, F.; Caliste, D.; Caracas, R.; Côté, M. ABINIT: First-principles approach to material and nanosystem properties. *Comput. Phys. Commun.* **2009**, *180*, 2582−2615.
(36) Blöchl, P. E. Projector augmented-wave method. *Phys. Rev. B* **1994**, *50*, 17953.
(37) Kresse, G.; Joubert, D. From ultrasoft pseudopotentials to the projector augmented-wave method. *Phys. Rev. B* **1999**, *59*, 1758.
(38) Bellunato, A.; Arjmandi Tash, H.; Cesa, Y.; Schneider, G. F. Chemistry at the Edge of Graphene. *ChemPhyschem* **2016**, *17*, 785−801.
(39) Wan, T.; Niu, D.; Wu, C.; Xu, F.-J.; Church, G.; Ping, Y. Material solutions for delivery of CRISPR/Cas-based genome editing tools: Current status and future outlook. *Mater. Today* **2019**, *26*, 40−66.
(40) Liu, C.; Luo, X. Potential molecular and graphene oxide chelators to dissolve amyloid-β plaques in Alzheimer's disease: a density functional theory study. *J. Mater. Chem. B* **2021**, *9*, 2736−2746.
(41) Liu, W.; Speranza, G. Tuning the oxygen content of reduced graphene oxide and effects on its properties. *ACS Omega* **2021**, *6*, 6195−6205.
(42) Yang, G.; Li, L.; Lee, W. B.; Ng, M. C. Structure of graphene and its disorders: a review. *Sci. Technol. Adv. Mater.* **2018**, *19*, 613−648.
(43) Larijani, H. T.; Ganji, M. D.; Jahanshahi, M. Trends of amino acid adsorption onto graphene and graphene oxide surfaces: a dispersion corrected DFT study. *RSC Adv.* **2015**, *5*, 92843−92857.
(44) Rossi-Fernández, A. C.; Villegas-Escobar, N.; Guzmán-Angel, D.; Gutiérrez-Oliva, S.; Ferullo, R. M.; Castellani, N. J.; Toro-Labbé, A. Theoretical study of glycine amino acid adsorption on graphene oxide. *J. Mol. Model* **2020**, *26*, 33.
(45) Krishnamoorthy, K.; Veerapandian, M.; Yun, K.; Kim, S.-J. The chemical and structural analysis of graphene oxide with different degrees of oxidation. *Carbon* **2013**, *53*, 38−49.
(46) Wilson, N. R.; Pandey, P. A.; Beanland, R.; Young, R. J.; Kinloch, I. A.; Gong, L.; Liu, Z.; Suenaga, K.; Rourke, J. P.; York, S. J. Graphene oxide: structural analysis and application as a highly transparent support for electron microscopy. *ACS Nano* **2009**, *3*, 2547−2556.
(47) Nakajima, T.; Matsuo, Y. Formation process and structure of graphite oxide. *Carbon* **1994**, *32*, 469−475.
(48) Hashemzadeh, H.; Raissi, H. Understanding loading, diffusion and releasing of doxorubicin and paclitaxel dual delivery in graphene and graphene oxide carriers as highly efficient drug delivery systems. *Appl. Surf. Sci.* **2020**, *500*, 144220.
(49) Wang, J.; Luo, X. Theoretical Investigation of the BCN Monolayer and Their Derivatives for Metal-free CO2 Photocatalysis, Capture, and Utilization. *ACS Omega* **2024**, *9*, 3772−3780.
(50) Bafekry, A. Graphene-like BC6N single-layer: Tunable electronic and magnetic properties via thickness, gating, topological defects, and adatom/molecule. *Phys. E* **2020**, *118*, 113850.
(51) Zhu, A.; Luo, X. Detection of COVID-19 through a heptanal biomarker using transition metal doped graphene. *J. Phys. Chem. B* **2022**, *126*, 151−160.

https://doi.org/10.1021/acsomega.4c08517
ACS Omega 2025, 10, 5593−5600